



# Evaluation of different levels of prestressing for cold forging tools by numerical simulation analysis

Fabricio Dreher Silveira<sup>1</sup> · Lirio Schaeffer<sup>2</sup>

Received: 14 March 2018 / Accepted: 15 June 2018  
© Springer-Verlag London Ltd., part of Springer Nature 2018

## Abstract

Cold extrusion is known as a metal forming process and used due to its dimensional precision. However, the process definition is obtained by empirical methods where experiments are performed previously and based on a “trial and error” method. To reduce costs, companies have been looking for the support of numerical simulation softwares with metal forming application. This study describes the investigation of the effect of different levels for prestressing of cold extrusion gear tool by using the software Simufact Forming. The dimensional deviations of the gear tooth were obtained from two numerical simulations and compared. The application of shrink rings for the prestressing of tooling was evaluated using two different methods to compare their efficiency. The first one is using conventional shrink rings with tool steel, while the second is the *stripwinding* concept developed by the company STRECON. To produce spur gears, the low carbon steel SAE 10B22 was used.

**Keywords** Finite element analysis · Cold extrusion · Gear accuracy · Shrink fitting · Stress-strain curves

## 1 Introduction

Extrusion is among the most representative plastic strain manufacturing processes in the industry because it allows the production of complex and precise geometries with great productivity. Despite these advantages, the productivity is in general connected to the use of a wide range of strain rates with direct influence in the raw material yield stress. Zhuang et al. [1] have checked in their studies that this is one of the main difficulties when working with numerical simulation of forming processes because usually the stress-strain curves of the raw material in the software database are not the same as the ones applied in the actual process. Based on their statement, testing is recommended to figure out the true yield stress of the raw material.

The finite element method can predict the extrusion industrial process and evaluate the process conditions or project

parameters as well. The results are used to improve project continuity and they can be tested and analyzed under several conditions in a short period of time, which represents savings because they are computational tests as the studies carried out by Hentz et al. [2] have shown. The first usage record of the term “finite element” was through Clough [3], being that the first developments of the finite element method occurred in the 50’s through the studies of Turner et al. [4]. The first applications of such method happened in the 1960s, which were used to structural analysis of manufacturing technologies and in the 1970s an alternative method called “flow formulation” was developed. This formulation characterizes the metal material flow after plastic deformation in an analogous manner to the flow of incompressible viscous fluids, which serves as the basis for several finite element softwares.

### 1.1 Objective and approach

This paper shows the study of a cold extrusion process by finite element analysis of a pinion which is applied in starter drive for automobiles. The software Simufact Forming was used to perform the numerical simulation. Its realistic prediction of the forming forces, while considering spring back effects and elasto-plastic material behavior, is necessary for a high precision simulation of cold forming processes. Elastic deformation of forging tools is deeply related to the dimension

✉ Fabricio Dreher Silveira  
fabricio.silveira@zensa.com.br

<sup>1</sup> R&D Department, ZEN S.A. Industria Metalurgica, 65 Guilherme Steffen, Brusque 88355-100, Brazil

<sup>2</sup> Laboratory of Metal Forming (LDTM), Universidade Federal do Rio Grande Sul, Porto Alegre 91509-900, Brazil

**Table 1** Chemical composition for SAE 10B22 steel

10B22 (wt%)	C	Mn	P	S	B
	0.18–0.23	0.70–1.00	Max. 0.030	Max. 0.050	0.0005–0.003

of the forged part. To predict dimensional changes in a forged part, the elastic deformation amount and behavior of the tool should be verified. With the development of the numerical analysis method, elastic and elasto-plastic deformation analysis was applied to obtain the stress distribution by Raddad and Kocanda [5]. Lee and Lee [6] made experimental and numerical analysis approaches to compare experimental deformation and numerical analysis results in cold forging tools. Overall tool deformation behaviors such as forging, unloading, and ejecting operations were investigated with the embedded strain gauge.

The aim of the analysis is to predict how the tooth gear will behave under different conditions of prestressing of the tool system. A practical experiment was carried out to compare the effect of different prestressing of cold extrusion tools and assistive technologies upon their respective products.

## 2 Materials and methods

### 2.1 Boron steel

The material which was used for this investigation to produce the forged component is the Boron steel SAE 10B22. This steel is produced by *Gerdau Aços Finos Piratini*, located in *Charqueadas*, Brazil, in wire rod, diameter 31.8 mm.

Boron steel is widely used to manufacture high strength bolts. The presence of low Boron content in steels with Carbon content in a range of 0.20% up to 0.40% allows to obtain an optimum average hardenability to meet the hardness and strength requirements, after quenching.

After the rolling process, the raw material is submitted to annealing. The wire drawing process is applied to meet the target diameter of 28.1 mm. Hardness and mechanical strength are important for the sequence of the production process. Table 1 shows the chemical composition for SAE 10B22.

The results of the mechanical properties of the material supplied such as hardness, tensile strength ( $\sigma_t$ ), and grain size (GS), as well as historical results for yield stress ( $k_{f0}$ ), area reduction (RA) and stretching ( $\delta$ ) after annealing are shown below.

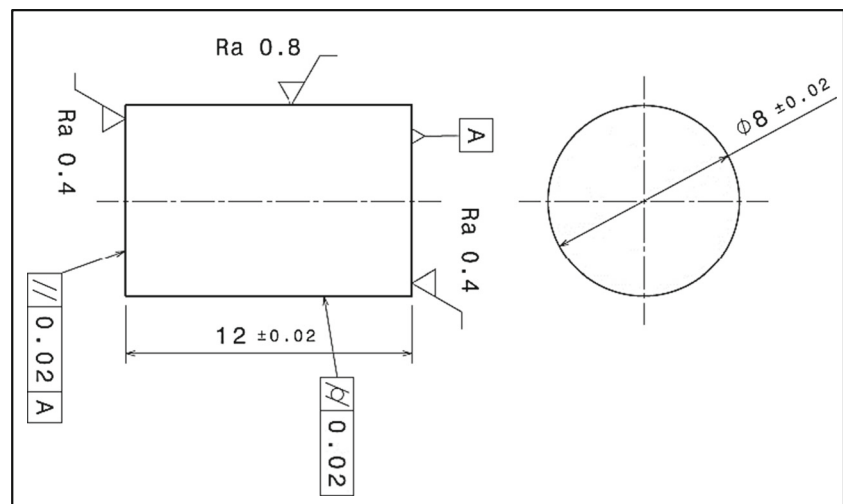
Hardness: max. 156;  $\sigma_t$ : max. 530 MPa;  $k_{f0}$ : 302 MPa; RA: 64%;  $\delta$ : 33%; GS: 5 up to 8.

### 2.2 Stress-strain curves

The thermomechanic inspection system Gleeble 3800 was used to plot the stress-strain curves of SAE 10B22 steel. Gleeble 3800 is capable of performing advanced thermo-mechanical experiments, such as high temperature tension/compression, torsion, and others. It allows to perform simple or complex thermo-mechanical treatment on conductive materials while accessing the material thermal, electrical and mechanical response, while phase transformations can be tracked using a dilatometer. Thus, Gleeble 3800 makes it possible to simulate materials processing conditions, such as cold and hot forming.

The tests were done at the *Institut für Umformtechnik (IFU)*, at Stuttgart University, Germany. The strain rate used was  $0.05 \text{ s}^{-1}$  at room temperature, 100, 200, 300, 400, and 500 °C. Three tests were performed for each temperature. The proof bodies were heated by conductive heating before being tested. The temperature of the samples was controlled by two

**Fig. 1** Proof body dimensions applied for tests in Gleeble 3800. According to DIN ISO 13175



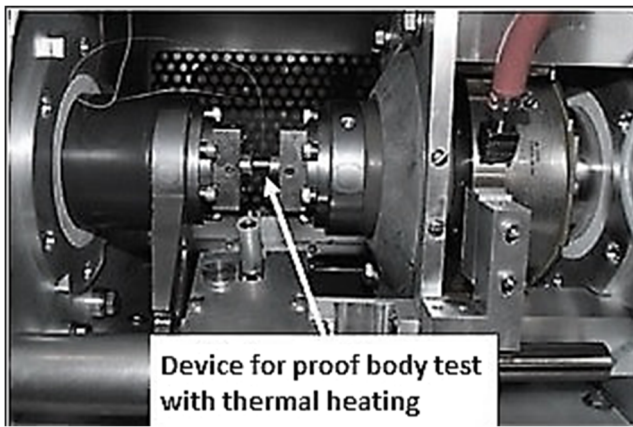


Fig. 2 Testing area of Geeble 3800 machine

thermocouples welded onto their surfaces. Figure 1 shows the dimensions of the proof body.

To minimize friction, strips of graphite were placed between the proof body and the forming punch of the machine. The heating rate was 15 °C/s for 10 s to ensure the temperature homogeneity of the samples. Elastic deformation of the machine was adjusted regarding the testing force. The stress-strain curves were calculated by using the diagram stroke × force and the proof body geometry. Considering the maximum true strain of 0.7, the stress-strain curve for room temperature was obtained according to the model developed by Hollomon-Ludwik [7], Eq. (1).

$$k_f = k_{f0} + C\varphi^n \tag{1}$$

where,  $k_f$  = true stress,  $k_{f0}$  = yield stress,  $C$  is the strength coefficient,  $\varphi$  is the true strain, and  $n$  is the strain hardening exponent. Figure 2 shows the testing area of the Geeble 3800 machine.

ASM (2002) and Drozda and Wick define the following values for the SAE 10B22 grade:  $k_{f0}$  = 193 MPa;  $C$  =

539 MPa;  $n$  = 0,261 [8, 9] for room temperature curve. Since the results for the compression test were obtained, they were used in Eq. (1) to plot the stress-strain curves.

Hensel and Spittel [10] describe the behavior of materials at high temperatures, which proposes the following model shown in Eq. (2).

$$k_f = k_{f0}A_1e^{-m_1T}A_2\varphi^{m_2}A_3\dot{\varphi}^{m_3} \tag{2}$$

where,  $A_1$  and  $m_1$ ,  $A_2$  and  $m_2$ ,  $A_3$  and  $m_3$  are modifying constants for temperature, strain and strain rate, respectively.

The stress-strain curves were plotted according to the calculated results and they are shown in the Fig. 3.

The scope of this study was based on a pinion which is applied to a starter drive for the original automotive Market. Such pinion has a 13-tooth gear, module 2.67 and it weighs 58 g. The dimensions of the pinion are shown in the Fig. 4.

### 2.3 Prestressing of tools

To compare the effect of different levels of prestressing of tools, the tooth deviations of gears produced by cold extrusion in a conventional double shrink ring tool and a stripwinding system, developed by the STRECON company, were investigated. The forged product was a pinion for starter drive different from that shown in Fig. 4, but also made in SAE 10B22 steel. This is a nine-tooth pinion with module 2.11 and lead length equal to 8 mm. Both tools had the same gear design for the die. The tools are shown in Fig. 5.

The conventional shrink ring tool has two shrink rings made in steel grades S1 and H13, which are the inner and outer ring, respectively. The interference fit is 0.3 mm for the inner ring and die. For the inner and outer ring, the interference fit is 0.25 mm. The average hardness was in a range of 56–58 HRc and 46–48 HRc. Yield strength for S1 is 2150 MPa and

Fig. 3 Stress-strain curves for SAE 10B22 steel. Strain rate 0.05 s<sup>-1</sup>. Source: IFU Stuttgart

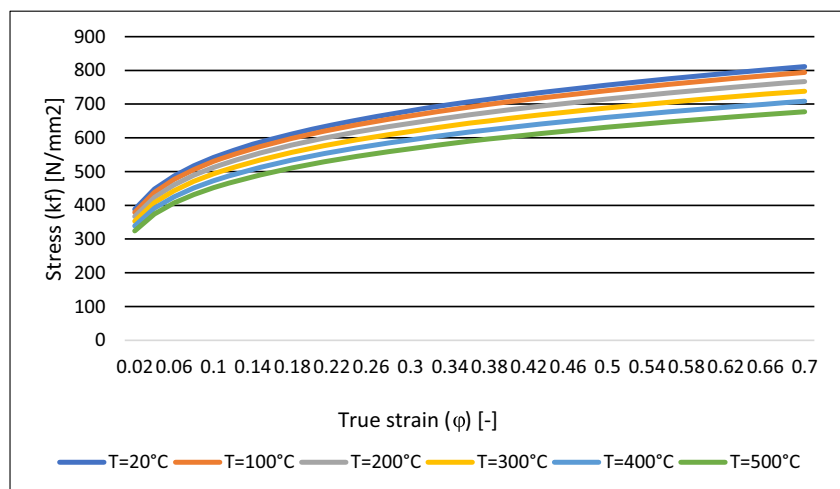
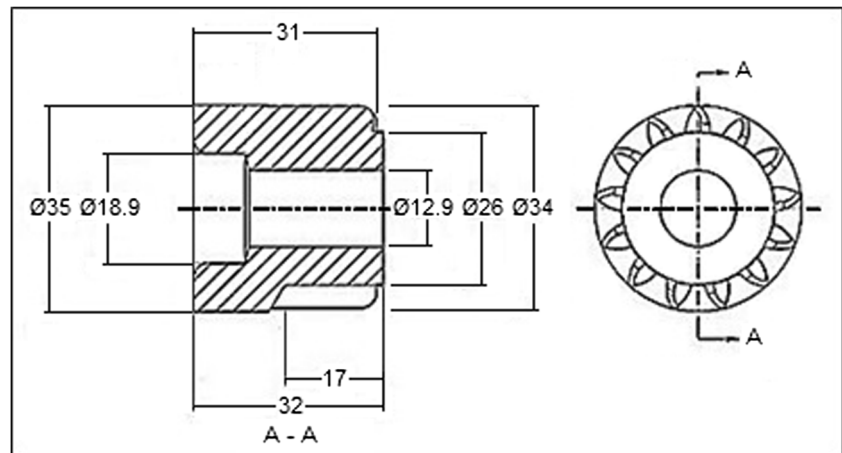


**Fig. 4** Drawing for cold extruded pinion



for H13 is 1380 MPa, for such hardness. The yield strength for the high-speed steel M2 applied in the dies is 3250 MPa.

The STRECON system is assembled with a shrink ring made by high strength steel strip by the stripwinding technique, which makes it stronger than conventional shrink rings. The yield stress of the steel strip is 2200 MPa at room temperature. Hardness is in a range of 62 up to 64 HRc. Considering tools with the same dimension, such system is twice as strong as a single shrink ring system and 1.7 times as strong as a double shrink ring system as Groenbaeck and Nielsen [11] researches demonstrate.

A more developed approach for prestressing is to look at the stress/strain behavior of the forging die. This approach examines the full load cycle of the forging die, including the stress range and the physical movement of the forging die (i.e., strain behavior). According to Lund et al. [12], the starting point of the forging die will be at a certain level of compressive stress, which is determined by the interference fit. The higher the level of prestressing, the higher the resulting compressive stress in the forging die. During the forging process of the part, the forging die would be heavily loaded and usually goes from a compressive state of stress into tensile stresses.

### 3 Experimental scope

The numerical simulation was carried out to determine the tooth flank profile of the gear after ejection from the die. The objective was to figure out the elastic tool behavior of the die and the effects on the forged product. For such simulation, the following data was used.

- 3D model of extrusion tool for starter drive pinion with 13 teeth.

- Tool velocity of 150 mm/s as it represents a mechanical press.
- Stroke equal to 25 mm which is determined by the dimensions of the pinion and die cavity.
- Elastic behavior of the workpiece and die was considered in the simulation.
- The software used for such numerical simulation was Simufact Forming V14. The structure of the tool can be seen in the cut view of the Fig. 6.

The workpiece for this simulation had a holed billet with the following dimensions:

$$\varnothing_{\text{outer}} = 32 \text{ mm}; \varnothing_{\text{inner}} = 13 \text{ mm}; \text{length} = 22.5 \text{ mm}$$

To investigate the behavior of the pinion after extrusion and ejection of the die, the tool was simplified. The two shrink rings of the original tool were exchanged by only one shrink ring. To reduce the time for simulation, one tooth of the 13 teeth used in the numerical analysis. The simulation setup where the parameters for simulation are established can be checked as follows.

Workpiece	Tools
<ul style="list-style-type: none"> <li>• Material: SAE 10B22;</li> <li>• Mesh: 107,000 elements;</li> <li>• Type: elastic-plastic;</li> <li>• Friction: <math>m = 0.12</math>;</li> <li>• Adaptive meshing;</li> <li>• 1/13 model (one tooth was simulated).</li> </ul>	<ul style="list-style-type: none"> <li>• Type: elastic;</li> <li>• Friction: <math>m = 0.12</math>;</li> <li>• Punch: 60,000 elements; Velocity: 150 mm/s; Stroke: 25 mm</li> <li>• Die: 164,000 elements; 1/13 model</li> </ul>

A friction factor of 0.12 is a common parameter for cold extrusion. Such friction factor was applied for the numerical simulation. After the finite element analysis of the pinion



**Fig. 5** Cold extrusion tooling used in the experiments. Conventional shrink rings (left). STRECON system (right)

extrusion, a force chart was created reflecting the efforts during the extrusion process. The simulation was concluded based on the stroke. Based on simulation results, a force of 1500 kN was necessary to produce the pinion with the stroke of 25 mm.

A second simulation was carried out aiming to evaluate the effect of shrink rings upon the die cavity and the results in the extruded product as deeply explored by Osakada [13]. The proposal was to consider the elastic behavior of the two shrink rings and it goes in the same direction of Lee et al. [14, 15] studies. Therefore, the original concept of the tool was applied. The interference fit of the inner shrink ring was increased in 0.03 mm between the dies and outer shrink ring, as well as, the prestressing of the tool. Figure 7 illustrates the points of adjustment.

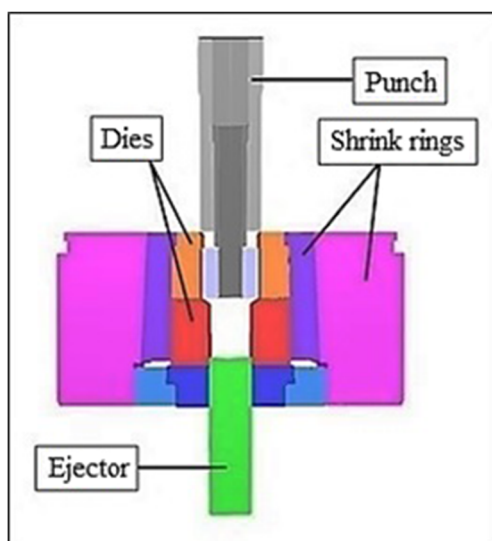


**Fig. 6** Cut view of cold extrusion tool used in the numerical simulation

The simulation setup is described as follows.

Workpiece	Tools
<ul style="list-style-type: none"> <li>• Material: SAE 10B22;</li> <li>• 75,000 elements;</li> <li>• Type: elastic-plastic;</li> <li>• Friction: <math>m = 0.12</math>.</li> <li>• Adaptive meshing.</li> </ul>	<ul style="list-style-type: none"> <li>• Type: elastic;</li> <li>• Friction: <math>m = 0.12</math>;</li> <li>• Punch: 45,000 elements;</li> <li>Velocity: 150 mm/s;</li> <li>Stroke: 25.7 mm</li> <li>• Upper die: 32,000 elements;</li> <li>• Lower die: 50,000 elements;</li> <li>• Inner shrink ring: 50,000 elements;</li> <li>• Outer shrink ring: 45,000 elements.</li> </ul>

Due to the elastic behavior of the tool after the interference fit adjustment, which was applied to the inner shrink ring, an internal displacement of 0.0247 mm could be observed in the die cavity. Figure 8 illustrates the radial displacement after simulation.

Regarding this FE analysis, the stroke of the punch was 25.7 mm, due to the greater prestressing of the tool, to meet the specification in length of the pinion. The aim is to reduce the range of tangential stresses in the inner surface of the die cavity by increasing the interference fit between the shrink rings, as well as, to lead the tool to a deep state of compressive stress. Since the level of prestressing of the tool is increased, the elastic strain behavior is changed, and it directly affects the amplitude of deviations applied in the extruded gear.

## 4 Results and discussion

The result analysis method is to compare the target pinion from the design of the 3D CAD project based on the die cavity

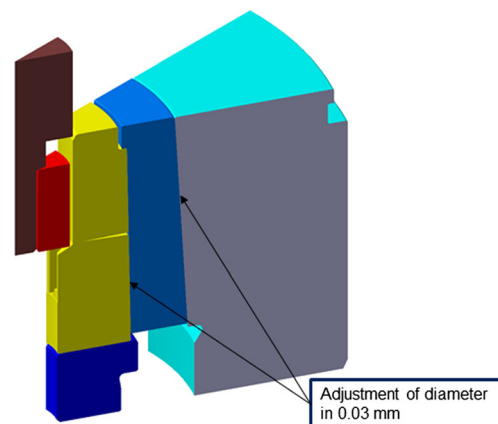


**Fig. 7** Adjustment of the inner shrink ring diameters for the second numerical simulation

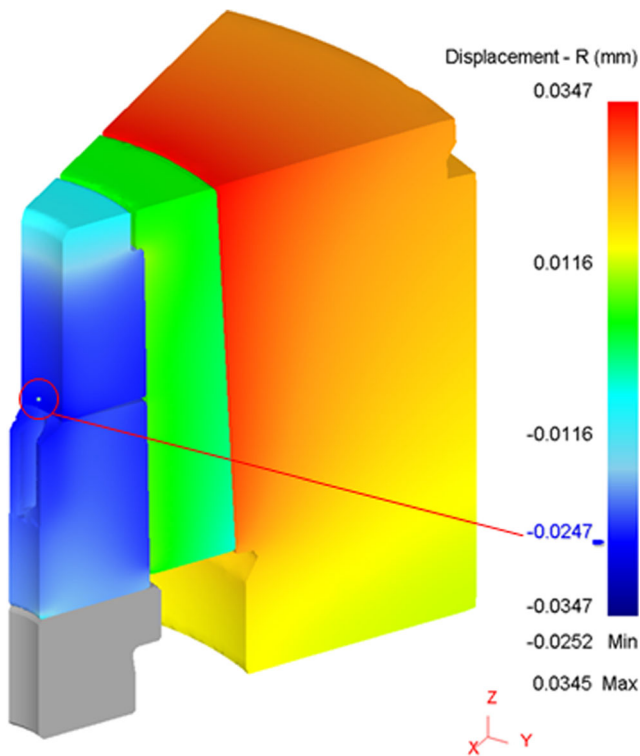
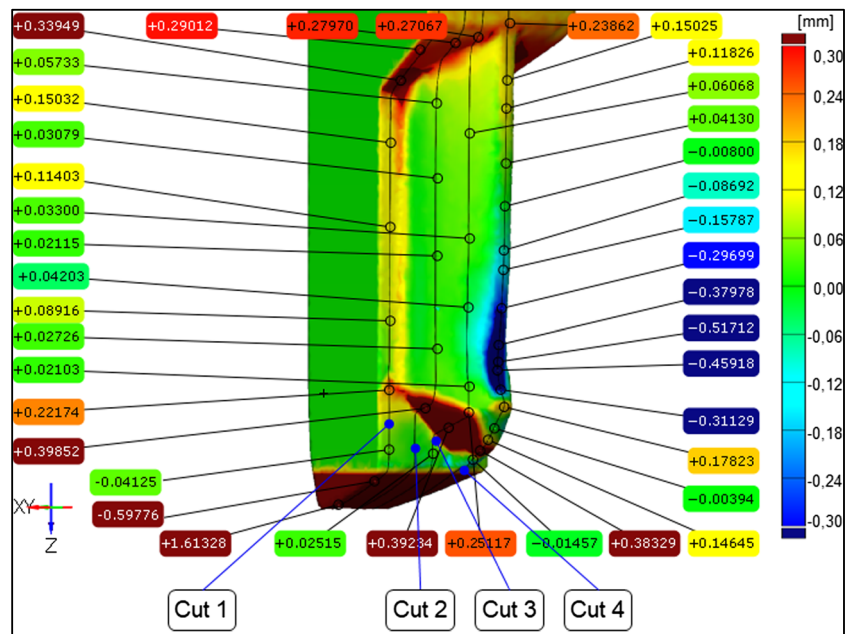


Fig. 8 Radial displacement after the interference fit of the tool

profile with the numerical simulation model result. Both models were overlapped referring to the cylindrical body of the pinion.

According to the results, the stroke of 25 mm did not form the tooth pinion. A sink on the top of the tooth occurred. It is a common failure due to two specific reasons based on recommendations of ASM [8].

Fig. 9 Dimensional deviations of pinion tooth after ejection of the die



- Insufficient stroke.
- The mass of the billet is not enough to meet all the requirements of the extrusion product.

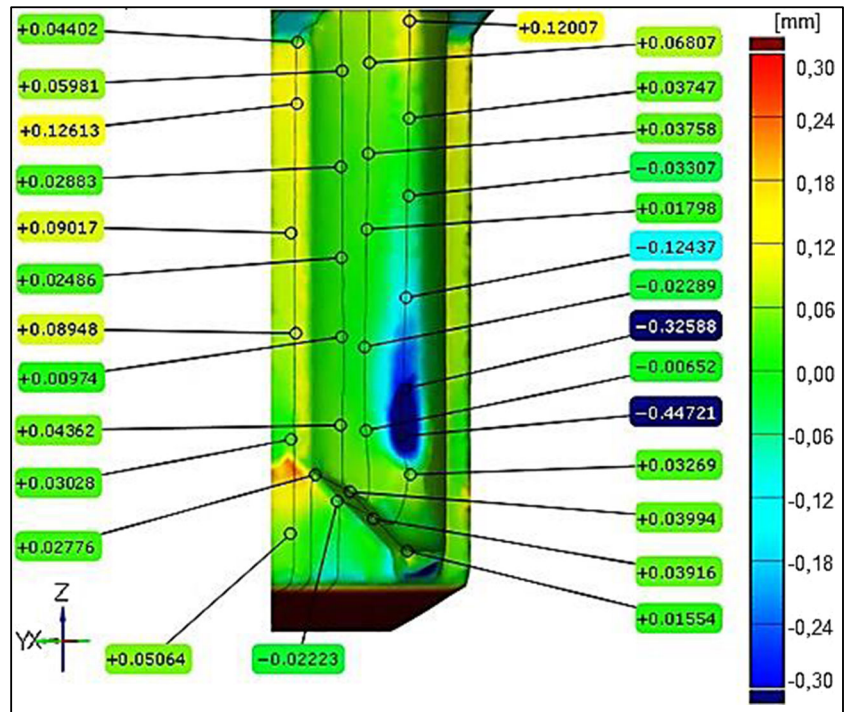
Regarding the first simulation, where the elastic behavior of the shrink rings was not considered, the dimensional deviations are demonstrated graphically in Figs. 9 and 10, respectively, for left and right side of the gear tooth.

In the results showed in Fig. 9, Cut 1 demonstrates an increasing deviation at the tooth base. Cut 2 reveals a high deviation at the lower area of the tooth where there is a chamfer. Such chamfer is produced at the bottom of the die cavity where the highest loads are concentrated after finishing the stroke of the punch. Both Cuts 2 and 3 show low deviation in the tooth flank. In Cut 4, there is a lack of material filling on the top of the tooth. The stroke of the punch could be increased to solve this failure model. However, Groenback and Hinsel [16] have proven that the efforts in the die cavity would also be increased and it could lead to early breakage of the tool.

The simulation with 25 mm of stroke showed a lack of filling on the top of the tooth, considering the calculated mass for the extruded part. Increasing the mass of the raw material could be a solution; on the other hand, the production cost would also be increased.

Regarding the results of the second simulation, the greater prestressing of the tool through the adjustment of the interference fit had a positive effect to minimize the dimensional deviations of the extruded gear, which complies with the numerical analysis carried out by Zhang et al. [17]. Figure 10 gives the results of the dimensional deviations of gear tooth. Comparing the results with those showed in the Fig. 9, it is

**Fig. 10** Dimensional deviations of pinion tooth after ejection of the die. After increased prestressing of the tool



possible to check a reduction upon the dimensional deviation after the ejection of the part from the die cavity, due to the higher prestressing.

The tooth deviation parameters of die cavities and their respective pinions were measured in a 3D machine by the software *Quindos Gear*. They are described as follows. Pinions can be seen in the Fig. 11.

$f_{H\alpha}$  = profile slope deviation;  $f_{f\alpha}$  = profile form deviation;  $F_{\alpha}$  = total profile deviation;  $f_{H\beta}$  = helix slope deviation;  $f_{f\beta}$  = helix form deviation;  $F_{\beta}$  = total helix deviation;  $f_{pt}$  = single pitch deviation;  $F_p$  = cumulative pitch deviation;  $F_r$  = radial runout;  $Q$  = gear accuracy grade.

Therefore, the chosen methodology for data acquisition was the measurement of each tooth flank for both right and left sides. The gear accuracy grade was evaluated according to



**Fig. 11** Pinions produced by cold extrusion with SAE 10B22 steel

the greater numeric result in a group of four consecutive flanks. According to ISO 1328-1, the lower the gear accuracy grade the better will be the accuracy of the involute profile. Both tools were tested in an eccentric press with 300-ton force with 47 strokes per minute. Tables 2 and 3 show the results of one sample produced by each tool.

Based on the results, it is possible to check that all the deviations of the forged products showed dimensional scatter. Individually, the die assembled in the STRECON container presented profile, helix, pitch and runout deviations lower than the die with conventional shrink rings. Thus, it means a more precise gear accuracy grade.

The elastic deformation difference between the numerical analysis and forged gear inspection can be caused from thermal deformation, which was not considered in this research. Differences between the material properties of the part and tool and friction conditions of lubricant can also be responsible for such changes in the result as Kang et al. [18] described in their studies in numerical simulation and practical experiments.

## 5 Conclusions and outlook

Regarding the aspects discussed in this investigation, it was possible to verify that the software Simufact Forming provided a wide range of process information to be analyzed. In order to find the best solution for the target process, parameters can be modified. In addition, it is necessary to be careful with the results obtained so that they are useful and consistent with the actual process. It is important to have the following

**Table 2** Gear flank deviations and accuracy grade of a forged pinion produced by conventional shrink rings tool

Left						Tooth deviation	Right					
<i>Q</i>	9 <i>X</i> (μm)	<i>Q</i>	8,7,6,5 <i>X</i> (μm)	<i>Q</i>	4,3,2,1 <i>X</i> (μm)		1,2,3,4 <i>X</i> (μm)	<i>Q</i>	5,6,7,8 <i>X</i> (μm)	<i>Q</i>	9 <i>X</i> (μm)	<i>Q</i>
9	13.5	10	18.1	10	19.1	$f_{H\alpha}$	20.0	10	21.4	10	20.4	10
9	23.2	10	27.7	10	27.0	$F_{\alpha}$	26.6	10	24.3	9	27.8	10
9	16.6	9	16.0	9	18.2	$f_{f\alpha}$	18.2	9	11.9	8	16.1	9
5	3.3	5	4.2	6	4.6	$f_{H\beta}$	5.7	6	5.7	6	3.5	5
6	6.2	8	13.5	7	11.7	$F_{\beta}$	133	8	24.3	7	7.0	6
6	4,3	8	11.6	8	9.0	$f_{f\beta}$	12.6	9	11.9	8	5.2	6
8			10.4			$f_{pt}$	11.0			8		
6			13.2			$F_p$	11.0			5		
9			29.7			$F_r^*$						

input data to be as close as possible to the reality of the process.

- Input the actual data of the target part for study.
- Tests to obtain the stress-strain curves of the raw material.
- To have knowledge of the resources available in the software.
- To understand and interpret the results from the simulation.

Softwares for numerical simulation are used for cost and development time reduction of a new product, as long as the cares cited above are taken. Numerical simulation has grown in the metal-mechanic industry even if the initial investment is high. The benefits brought by exchanging the “trial and error” method compensate the acquisition of such tool as this one.

The numerical simulation was run to verify the effect of the shrink rings in the extruded gear. After the second simulation, where an increase in the compressive stress state of the tool was applied due to a greater interference fit, the elastic

behavior of the extruded part was modified according the dimensional deviations results. Based on the simulation results, the more precise the shrink rings dimensioning is, the greater dimensional quality of the extruded product will be presented.

The results in Tables 2 and 3 showed a significant difference between the quality of the cold forged gears. The residual stresses and tool elastic deformation, which applies a plastic deformation to a forged product, are some of the main points that affect the gear accuracy grade of the pinion.

According to the results, one can see that all deviations of the forged products showed dimensional scatter regarding the results found in their respective dies. Individually, the die assembled in the STRECON container presented profile, helix, pitch and runout deviations lower than the die with normal shrink rings. Therefore, it means a more precise gear accuracy grade. An alternative approach to obtain high-stiffness forging tools would be to integrate the tungsten carbide material as part of the prestressing

**Table 3** Gear flank deviations and accuracy grade of forged pinion produced by the STRECON tool

Left						Tooth deviation	Right					
<i>Q</i>	9 <i>X</i> (μm)	<i>Q</i>	8,7,6,5 <i>X</i> (μm)	<i>Q</i>	4,3,2,1 <i>X</i> (μm)		1,2,3,4 <i>X</i> (μm)	<i>Q</i>	5,6,7,8 <i>X</i> (μm)	<i>Q</i>	9 <i>X</i> (μm)	<i>Q</i>
9	14.8	10	23.4	10	20.5	$f_{H\alpha}$	24.4	11	24.1	11	20.5	10
9	22.4	10	28.5	10	27.1	$F_{\alpha}$	32.2	10	28.7	10	25.1	9
8	13.7	8	11.1	8	11.8	$f_{f\alpha}$	11.6	8	11.4	8	11.6	8
2	1.1	3	1.6	2	1.1	$f_{H\beta}$	2.1	3	2.0	3	1.4	2
4	3.8	7	11.2	6	8.2	$F_{\beta}$	12.6	8	8.6	7	3.2	4
4	2.7	8	11.0	8	8.5	$f_{f\beta}$	11.9	8	9.6	8	3.1	5
5			4.6			$f_{pt}$	3.5			4		
3			5.0			$F_p$	5.7			4		
6			9.1			$F_r^*$						

system, for example by having the inner ring of the double ring system made of tungsten carbide.

The cold forged pinions produced by both tooling systems showed similar profile deviation. However, helix, pitch, and runout deviation had better performance for pinions produced by the STRECON container die. The gear accuracy grade was more effective for these deviations.

**Acknowledgements** The authors gratefully acknowledge the support of ZEN S.A. *Industria Metalurgica* that made the software Simufact Forming available and data acquisition by practical tests with tooling and forging presses, and the *Metal Forming Institute of Stuttgart University* for the experiments carried out with the raw material which was scope of this research.

## Compliance with ethical standards

**Conflict of interest** The authors declare that they have no conflict of interest.

**Publisher's Note** Springer Nature remains neutral with regard to jurisdictional claims in published maps and institutional affiliations.

## References

- Zhuang, W.; Han, X.; Hua, L.; Differences between traditional cold forging and cold orbital forging of a spur bevel gear, International Conference on the Technology of Plasticity, ICTP 2017, September 2017, Cambridge, UK
- Hentz, E. A.; Schaeffer, L.; Knoll, P. K.; *Influência da Curva de Escoamento na Simulação Computacional do Processo de Forjamento a Quente da Liga de Titânio Ti-6Al-4v*. *Ciência & Engenharia*, v. 16, n. 1/2, p. 53–59, jan. - dez. 2007
- Clough, R.; *The Finite Element Method in Plane Stress Analysis*. In: *Anais da 2. Conference on Electronic Method. International Computation.* 1960, Pittsburgh: American Society of Civil Engineers. p. 345–378
- Turner, M.; Clough, R.; Martin, H.; Topp, I.; Stiffness and deflection analysis of complex structures. *J Aeronautical Sci*, v. 23, n. 9. p. 805–821, setembro 1956, 823
- Raddad, B.; Kocanda, A.; On the strength criteria for high stressed ring-shaped dies, in: *Proceedings of the fourth international conference on Technology of Plasticity*, 1993, pp. 5–9
- Lee YS, Lee JH (2004) Finite element modeling approaches to the accurate dimensional prediction for a cold-forged part. *J Eng Manuf* 218:1709–1722
- Hollomon, J. H.; *Tensile deformation*. Transactions—American Institute of Mining and Metallurgical Engineers, New York, v. 126, p. 268–290, 1945
- ASM HANDBOOK; *Failure Analysis and Prevention*; ASM International, vol. 11, 2002
- Drozda, T. J.; Wick, C., *Tool and manufacturing engineers' handbook*. 4. Ed. Dearborn: Society of Manufacturing Engineers, 5 v, 1983
- Hensel, A, Spittel, T.; *Kraft- und Arbeitsbedarf bildsamer Formgebungsverfahren*, Leipzig: VEB Deutscher Verlag für Grundstoffindustrie, 1978, p. 200–202
- Groenbaeck J, Nielsen EB (1994) New developments in the design of high performance, stripwound cold forging tools. *J Mater Process Technol* 46:87–97
- Lund, E.; Andresen, H.; Jepsen, C.; *Tool optimization by means of effective prestressing system, STRECON A/S, Sonderborg, Denmark*, 2015
- Osakada, K.: *Cold forging in Japan*, Presentation at the 40th International Cold Forging Group, Plenary Meeting, Padova, Italy, September 2007
- Lee YS, Lee JH, Ishikawa T (2002) Analysis of the elastic characteristics at forging die for the cold forged dimensional accuracy. *J Mater Process Technol* 130/131:532–539
- Lee YS, Lee JH, Choi JU, Ishikawa T (2002) Experimental and analytical evaluation for elastic deformation behaviors of cold forging tool. *J Mater Process Technol* 127:73–82
- Groenbaeck, J.; Hinsel, C.; *Improved Fatigue Life and Accuracy of Precision Forging Dies by Advanced Stripwound Prestressing System*, SME Clinic on Precision Forging Technology, Columbus, Ohio, USA, Nov 10, 2000
- Zhang, Y.; Huang, J.; Lin, X.; Quanshui, F.; Numerical simulation analysis on cold closed-die forging of differential satellite gear in car, *materials science forum*, Vols 575-578 (2008) pp 517–524
- Kang JH, Lee KO, Je JS, Kang SS (2007) Spur gear forging tool manufacturing method considering elastic deformation due to shrink fitting. *J Mater Process Technol* 187-188:14–18